

The structural properties of liquid and quenched sulphur II

This article has been downloaded from IOPscience. Please scroll down to see the full text article.

1994 J. Phys.: Condens. Matter 6 3619

(<http://iopscience.iop.org/0953-8984/6/20/002>)

View [the table of contents for this issue](#), or go to the [journal homepage](#) for more

Download details:

IP Address: 171.66.16.147

The article was downloaded on 12/05/2010 at 17:37

Please note that [terms and conditions apply](#).

The structural properties of liquid and quenched sulphur II

M Stolz[†], R Winter[†], W S Howells[‡], R L McGreevy[§] and P A Egelstaff^{||}

[†] Institute of Physical Chemistry, University of Dortmund, D-44227 Dortmund, Germany

[‡] Rutherford Appleton Laboratory, Didcot, Oxon OX11 0QX, UK

[§] Studsvik Neutron Research Laboratory, S-611 82 Nyköping, Sweden

^{||} Physics Department, University of Guelph, Guelph, Ontario N1G 2W1, Canada

Received 20 December 1993, in final form 11 February 1994

Abstract. Neutron diffraction experiments over the momentum transfer range $0 < Q$ (\AA^{-1}) < 40 have been used to investigate the structural properties of liquid sulphur from 140 °C up to 300 °C, i.e. from conditions near the melting point of sulphur up to temperatures well above its λ -transition ($T_\lambda = 159$ °C), and to study how the structure of sulphur rapidly quenched from different liquid temperatures changes in relation to the corresponding liquid structure. The data have been Fourier transformed to give an accurate pair correlation function $g(r)$ from which absolute numbers and distances of atoms in given molecular configurations may be obtained. The results indicate which molecular bonds are changed in the different solid and liquid states and shed new light on the λ -transition from a molecular point of view. In particular we show that the number of nearest neighbours probably increases with temperature above the λ transition. The data on $g(r)$ are also interpreted with recent reverse Monte Carlo calculations.

1. Introduction

The investigation of elemental sulphur offers an attractive challenge because of the unique diversity of stable molecules that it can form in the gaseous, liquid and solid state and because the chemical conversions of molecular species occur at moderate temperature and pressure conditions [1, 2]. The stable crystalline modification at room temperature is orthorhombic sulphur (α -S). The structure is based on the packing of puckered S_8 rings as structural units with an average bond length of 2.05 Å, and exactly 2.0 nearest neighbours. At about 95 °C, α -S converts into monoclinic β -S, which melts at 119 °C. It is reported that the liquid is made up mainly of S_8 ring molecules, too [1, 2]. At 159 °C a phase transition occurs in the melt, which is indicated, for example, by a drastic increase of the viscosity [1–3]. This so-called λ -transition has been interpreted as being mainly due to the conversion of S_8 rings to long polymer chains [1, 2].

The local structure of S in its liquid and quenched states has attracted considerable experimental as well as theoretical attention for many decades [1, 4–15]. However, no model yet accounts satisfactorily for all its properties. To obtain a better understanding of this system, we have performed a series of accurate diffraction experiments. Here, we describe the results on liquid S in the temperature range of 140–300 °C, i.e. at conditions around the λ -transition, and on quenched and polymeric S. In order to obtain good real-space resolution it was necessary to measure the structure factors, $S(Q)$, of the samples up to high momentum transfers and therefore pulsed neutron diffraction experiments were carried out. These experiments are both a continuation of and an improvement upon our earlier work [10] using pulsed neutron beams.

2. Experimental method

The S samples of 99.999% purity were contained in a cylindrical vanadium cell having an inside radius of 15 mm and a wall thickness of 0.1 mm. After filling with S, the cell for measurements of the liquid states was outgassed and then sealed by electron beam welding. The temperature of the cell was adjusted by two independent resistance heaters mounted below and above the neutron beam height and controlled to within ± 0.1 °C.

The quenched S samples were obtained by rapidly ejecting molten S from a syringe into liquid nitrogen. For the preparation of pure polymeric S, the quenched S samples were eluted several times with liquid carbon disulfide (CS₂) at room temperature.

The pulsed neutron diffraction experiments were carried out using the SANDALS (for the liquid S samples) and the LAD instrument (for the quenched S samples) located at the ISIS pulsed neutron facility at the Rutherford Appleton Laboratory, Chilton, UK. The measured scattering intensities were corrected for background, absorption, multiple scattering and inelasticity using the ATLAS program package developed at the RAL. The differential scattering cross sections were normalized to an absolute scale by comparing the sample's scattering intensity with that of a standard V sample. These data on $d\sigma/d\Omega$ are related simply to the liquid or amorphous structure factor, $S(Q)$, and the liquid or amorphous pair correlation function, $g(r)$, by the formula

$$d\sigma/d\Omega = b^2 S(Q) = b^2 \left[1 + \rho \int_V [g(r) - 1] e^{iQ \cdot r} d\tau \right] \quad (1)$$

where b is the nuclear scattering amplitude for sulphur. To obtain high resolution in real-space correlation functions, data out to momentum transfers of 40 \AA^{-1} were Fourier transformed using standard methods.

The calorimetric measurements on quenched S samples were carried out using a Perkin-Elmer DSC7 differential scanning calorimeter. The S samples, quenched into liquid nitrogen, were filled at about -100 °C into large DSC volume capsules, which contain about 50 mg of sample and are made from stainless steel with O-ring sealing. In the thermogram, the difference ΔP between the heat flow into the S sample and a blank is plotted versus increasing temperature. ΔP is proportional to the specific heat c_p of the sample. We used a programmed constant heating rate of 2 °C min^{-1} in the DSC experiment.

3. Experimental results and analysis

3.1. Liquid sulphur

Figure 1 depicts the measured molecular structure factor $S(Q)$ of liquid S at 140 °C, 170 °C and 300 °C, i.e. at conditions below and above the λ -transition, measured at SANDALS. As can be clearly seen, the first maxima are composed of a shoulder at $Q_1 = 1.2 \text{ \AA}^{-1}$ and peaks at $Q_2 = 1.74 \text{ \AA}^{-1}$ and $Q_3 = 4.04 \text{ \AA}^{-1}$. Their positions remain essentially constant with increasing temperature, but the relative intensities $S(Q_1)$ and $S(Q_2)$ change with increasing temperature, as is illustrated in figure 2. No abrupt changes are observed at the λ -transition, although we have observed minor changes in the slope of $S(Q_1)$ and $S(Q_2)$ versus temperature in a detailed study of the temperature dependence of the height of the first two peaks of $S(Q)$ [9]. The structure of the peaks above $Q = 3 \text{ \AA}^{-1}$ smooths out with increasing temperature; for example, the weak shoulder of the broad peak at Q_3 for $T = 140$ °C has disappeared at $T = 300$ °C. We further note that little temperature

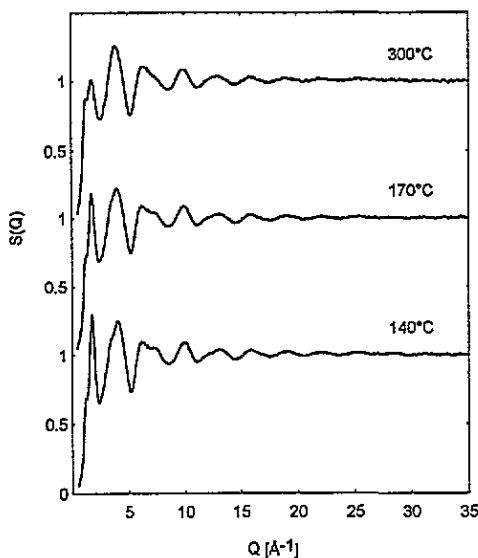


Figure 1. The molecular structure factor $S(Q)$ of liquid S at 140 °C, 170 °C and 300 °C (the corresponding number densities are $\rho = 0.0335 \text{ \AA}^{-3}$, $\rho = 0.0332 \text{ \AA}^{-3}$ and $\rho = 0.0318 \text{ \AA}^{-3}$).

dependence of $S(Q)$ is seen at $Q > 4 \text{ \AA}^{-1}$, which indicates that to a first approximation the short-range order of the S molecules does not change markedly in the whole temperature range covered.

The data were then Fourier transformed to the pair correlation function $g(r)$ (see figure 3). From these data it is obvious that the structural changes accompanying the λ -transition are very small. Each of the $g(r)$ curves shows about two nearest neighbours centred around 2.06 \AA , a second concentration of roughly three atoms at a distance of about 3.3 \AA , and a third peak for the liquid around 4.45 \AA which is broad and decreases in height with increasing temperature.

Comparing our data with earlier measurements of $S(Q)$ of liquid S [5–9] using x-ray and neutron diffraction techniques, which have been performed over a much smaller Q -range, we note some significant differences, especially in the intermediate r -range. This demonstrates the necessity of reaching high Q -values in diffraction experiments on molecular liquids.

The mean number of nearest neighbours has been obtained by (i) a Gaussian fit to the first peak of $g(r)$ and (ii) integration between the minima around the first peak in $g(r)$; the data are shown in table 1. For models such as S_8 rings and for long freely rotating chains, which have been proposed as models (see, e.g., [1, 2]) for liquid S below and above the λ -transition, respectively, the first peak in the distribution function should contain 2.0 atoms at 2.06 \AA . However, the peak observed experimentally at $r_1 = 2.06 \text{ \AA}$ contains less than two atoms within the S molecules for all temperatures, including $T < T_\lambda$, as can be seen from table 1. This indicates that the local liquid structure is broken up compared to the crystalline case for all temperatures.

As shown in table 1, the distance r_2 of the next-nearest neighbours is centred around 3.3 \AA . The intramolecular next-nearest-neighbour distance of S_8 rings or of S chains is 3.3 \AA and the corresponding peak in $g(r)$ should contain two atoms. Therefore, the additional one atom centred at 3.3 \AA (see table 1) has to be attributed to a neighbouring S molecule (in crystalline α - S_8 , the first intermolecular distance occurs around 3.38 \AA). Interestingly,

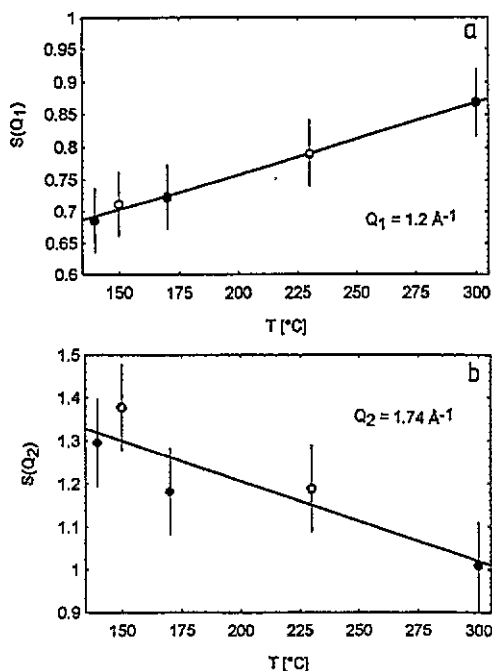


Figure 2. The height of the first two peaks of $S(Q)$ as a function of temperature (open circles: previous LAD data [10]).

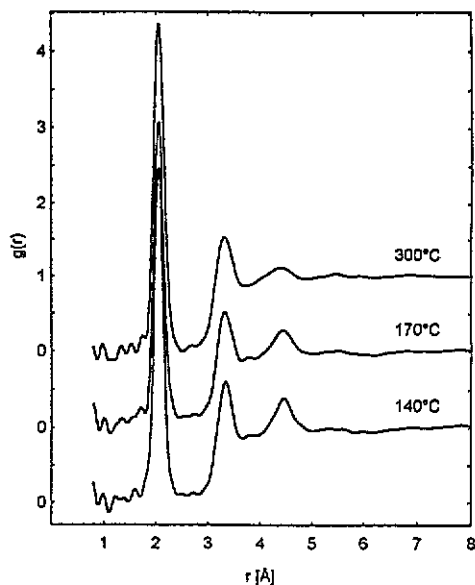


Figure 3. The pair correlation function $g(r)$ of liquid S at 140 °C, 170 °C and 300 °C.

Table 1. A summary of the lowest two peaks in $g(r)$ (r_1 , r_2 , mean first- and second-neighbour distances; N_1 , N_2 , mean first- and second-neighbour coordination numbers; obtained from (i) a Gaussian fit to the first peak of $g(r)$ and (ii) integration between the minima around the first peak in $g(r)$).

T (°C)	r_1 (Å)	r_2 (Å)	N_1 (i)	N_1 (ii)	N_2 (i)
140	2.053 ± 0.003	3.335 ± 0.01	1.71 ± 0.1	1.80 ± 0.1	3.2 ± 0.2
150 ^a	2.056 ± 0.003	3.325 ± 0.01	1.84 ± 0.1	1.86 ± 0.1	2.9 ± 0.2
170	2.053 ± 0.003	3.315 ± 0.01	1.68 ± 0.1	1.78 ± 0.1	3.0 ± 0.2
230 ^a	2.057 ± 0.003	3.310 ± 0.01	1.82 ± 0.1	1.88 ± 0.1	2.8 ± 0.2
300	2.054 ± 0.003	3.310 ± 0.01	1.85 ± 0.1	1.87 ± 0.1	3.1 ± 0.2

^a Previous LAD data [10].

r_2 might decrease slightly with increasing temperature, which means that the intermolecular distances in this temperature range are even slightly shorter at higher temperatures, perhaps due to closer intermolecular packing.

It is worthwhile investigating the temperature dependence in greater detail by calculating the difference function

$$\Delta(\rho g(r))/\rho_1 = [\rho_1 g_1(r) - \rho_2 g_2(r)]/\rho_1 \quad (2)$$

where the subscripts (1,2) refer to experiments at temperatures T_1 and T_2 . This may be calculated directly by Fourier transforming the difference in $S(Q)$ factors (see equation (1)). This quantity is related to the changes ΔN in the numbers of atoms in a spherical annulus

(extending from $r = r_1$ to $r = r_2$) through the equation

$$\Delta N(r_1, r_2) = 4\pi \int_{r_1}^{r_2} r^2 \Delta(\rho g(r)) dr. \quad (3)$$

Data of high precision are required to evaluate $\Delta(\rho g(r))$, and we show an informative example in figure 4, for $T_1 = 300^\circ\text{C}$ and $T_2 = 170^\circ\text{C}$. The three peaks in figure 3 are seen, through figure 4, to vary with increasing temperature in an interesting way: the first peak increases, the second peak broadens and the third peak decreases with temperature. The most likely explanation of this unusual behaviour is that the intramolecular peaks at 2.06 and 3.3 Å increase in area and remain sharp, while the intermolecular peaks at 3.3 Å and 4.45 Å broaden and decrease in amplitude with increasing temperature.

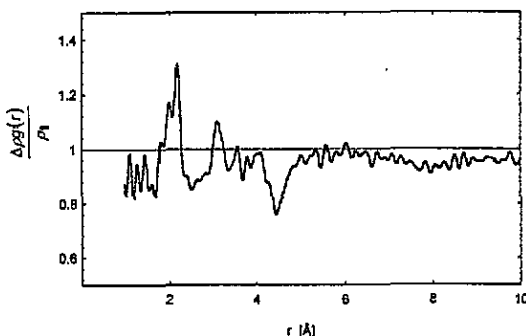


Figure 4. The difference pair correlation function $\Delta(\rho g(r))/\rho_1$ of equation (2) for $T = 300^\circ\text{C}$ and 170°C .

3.2. Quenched sulphur

We have shown by neutron diffraction experiments at D4B (Institut Laue Langevin, Grenoble), that a truly amorphous solid form of S can be made by quick quenching liquid S from the quenching temperature $T_q = 230^\circ\text{C}$ into liquid nitrogen [15]. A translucent glass is obtained, whose structure factor is similar to that for the parent liquid. The only difference is that the small shoulder in the liquid curve at 1.2 \AA^{-1} is hardly seen and the broad peak at about 6.5 \AA^{-1} has developed into a doublet in the amorphous curve. In the recent experiment at LAD, two quenched S samples have been measured at liquid nitrogen temperature (-196°C) after quenching from the quenching temperatures $T_q = 250^\circ\text{C}$ and $T_q = 140^\circ\text{C}$ (figure 5). For $T_q = 250^\circ\text{C}$, the experimental $S(Q)$ is similar to that of the sample quenched from 230°C and measured at D4B (see figure 5).

In the case of $T_q = 140^\circ\text{C}$, besides the underlying diffraction pattern of the frozen disordered melt, a superposition of Bragg reflections appears (see figure 5). This partially amorphous state for $T_q = 140^\circ\text{C}$ has been observed for the first time by diffraction experiments and it may be possible to suppress the partial crystallization by a still faster quenching process. The structure of the partially crystallized phase of the quenched product cannot be attributed to one of the well known stable crystalline S compounds such as orthorhombic $\alpha\text{-S}_8$ or monoclinic $\beta\text{-S}_8$.

A comparison between the pair correlation functions of the quenched S states and the parent liquid (figure 6) shows that significant differences occur in the intermediate-range

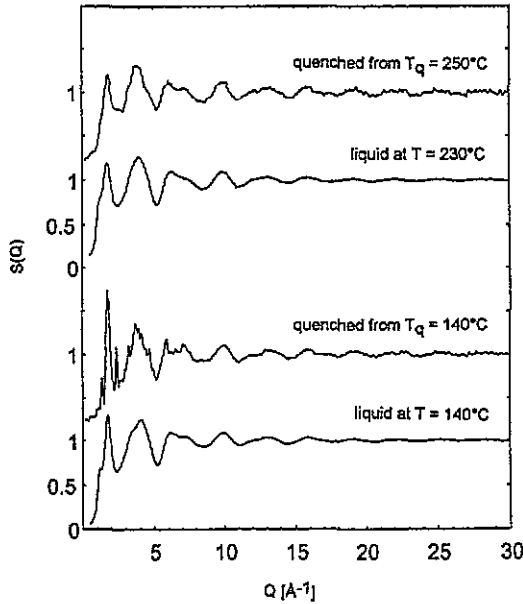


Figure 5. A comparison of $S(Q)$ for quenched and liquid S.

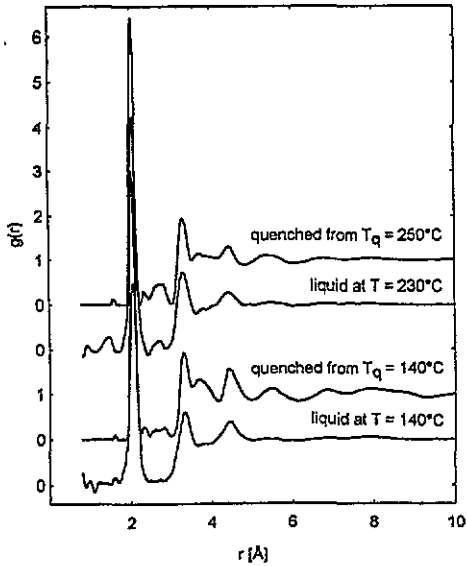


Figure 6. A comparison of $g(r)$ for quenched and liquid S.

order. The half widths of the nearest-neighbour peaks in $g(r)$ are smaller in the quenched state, as expected. In the region of $r = 2.7 \text{ \AA}$, the quenched material seems to have more intensity than the corresponding liquid it was quenched from. This indicates, that there might be more broken bonds in the solid quenched state with distances in the range between the first- and second-nearest-neighbour shells, especially in the case of $T_q = 250^\circ\text{C}$.

Furthermore, around $r = 3.7 \text{ \AA}$, broad peaks in $g(r)$ of the quenched samples develop, which indicates a stronger ordering of adjacent S molecules at this distance in the solid material. This effect is more pronounced for the sample quenched from $T_q = 140^\circ\text{C}$, which suggests that it might be more ordered over a larger range in the liquid state, and we note that a peak near 3.7 \AA is seen in the α -crystalline sample (figure 9).

3.3. Polymeric sulphur

Figure 7 exhibits a DSC scan of S quenched from 250°C into liquid nitrogen. A step in the DSC trace is clearly visible at about -25°C which is characteristic of a glass transition. At this temperature, the amorphous S structure changes again. The material first becomes extremely elastic (plastic S) and then begins to lose its rubbery properties due to a process of crystallization, and a mixture of crystalline polymeric and α -S₈ is obtained. This material has a half life of 46 d at room temperature [9].

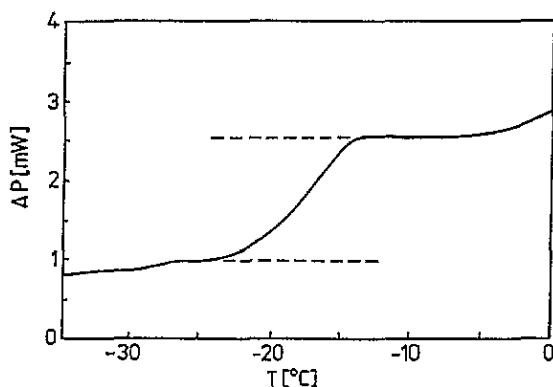


Figure 7. A DSC scan of S quenched from 250°C into liquid nitrogen.

When amorphous S, quenched to -196°C from a temperature above the λ -transition of the melt and warmed to room temperature, is dissolved in liquid CS₂, a residue is obtained, which consists of a crystalline material called polymeric S (ω -S). Figure 8 shows its structure factor, measured at room temperature at LAD. The diffraction pattern exhibits a few Bragg reflections and is thus different from the $S(Q)$ of the liquid and the amorphous state, and it is also different from the $S(Q)$ of crystalline α -S₈, the stable compound at room temperature. According to the literature [1, 2] extraction of the smaller S species by dissolution in CS₂ allows the long S chains to order. X-ray diffraction data for stretched fibres of plastic S suggested [1, 2] that this material might consist of close-packed helices, having nearly 10 atoms of S in three turns. However, there is still some doubt about the precise geometry of the chains, and the exact way in which they pack together.

Figure 9 shows the $g(r)$ of polymeric S in comparison to the $g(r)$ of the amorphous and α -S₈ samples. The major differences between the $g(r)$ of the polymeric and the other samples shown are changes in the medium-range order between 3.5 \AA and 5 \AA and a new broad intermolecular peak appearing at 6.5 \AA in the polymeric sample. This suggests that the long S chains are probably more ordered in ω -S than in the glass.

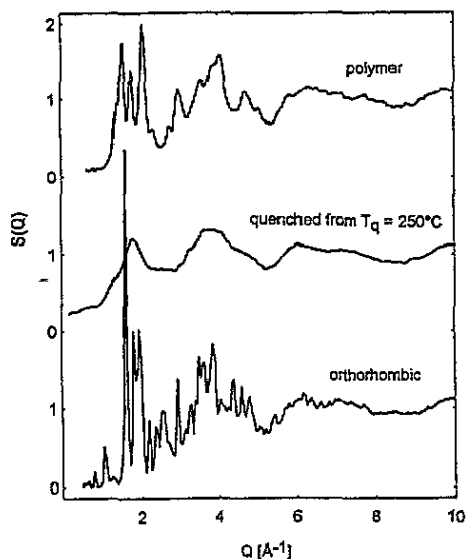


Figure 8. A comparison of $S(Q)$ for polymeric, quenched and crystalline α -S.

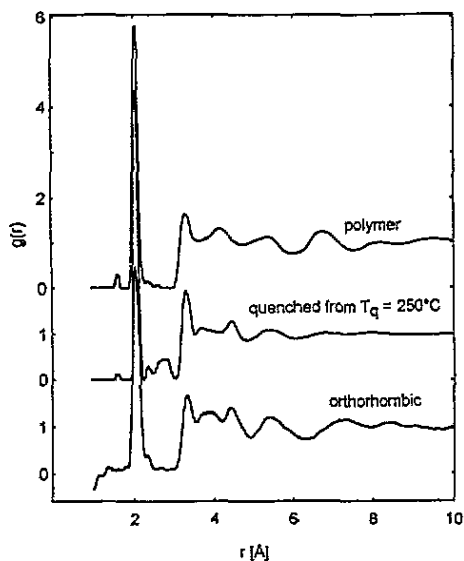


Figure 9. A comparison of $g(r)$ for polymeric, quenched and crystalline α -S.

4. Interpretation using the reverse Monte Carlo method

The reverse Monte Carlo (RMC) method has been described in detail elsewhere (see, e.g., [16]). Briefly, a structural model is modified, by a Monte Carlo method, to produce close agreement with the available experimental diffraction data. One starts with an initial configuration, which is a three-dimensional array of N points (atoms) in a cube of side L . L is chosen such that the density N/L^3 is equal to the experimental number density.

Normal periodic boundary conditions are applied, and $g(r)$ and $S(Q)$ are calculated from the configuration. Then, a new configuration is generated by random motion of one point. The new pair correlation function $g'(r)$ and structure factor $S'(Q)$ are calculated, as are the differences χ^2 and χ'^2 between the experimental and calculated structure factors. If $\chi^2 > \chi'^2$, then the move is accepted. If $\chi^2 < \chi'^2$, then the move is accepted with probability $\exp(\chi^2 - \chi'^2)$, otherwise the move is rejected and the configuration is changed back to its previous state. These steps are repeated until χ^2 is sufficiently small and oscillates around an equilibrium value. At this point, the configuration that corresponds to a $S(Q)$ that agrees with the experimental $S(Q)$ within experimental error can be evaluated.

In the case of S, we have made models composed of (i) rigid crown-shaped S_8 molecules (with an appropriate Debye-Waller factor fitted to the high- Q structure factor), (ii) flexible S_8 molecules, (iii) short chains and (iv) long chains. Models of types (ii), (iii) and (iv) all fit both high- and low-temperature liquid structure factors extremely well. As an example, figure 10 gives the RMC result of model (ii) for liquid S at 140°C. Model (i) does not fit as well. To obtain a reasonable fit with this model it is necessary to allow the shortest intermolecular distance to be 2.3 Å, that is, only slightly larger than the S-S bond. If a distance of 3 Å is chosen, that is, the beginning of the second peak in $g(r)$, the fit is poor. This shows that a liquid composed entirely of rigid S_8 molecules is not consistent with the data. It also shows that the fact that $g(r)$ does not fall to zero between the first and second peak, but rather has a small finite value, is significant. The failure of model (i) can also be traced to the absence of a third peak in $g(r)$ around 3.9 Å, corresponding to the third-neighbour distance across the S_8 ring. Such a peak does occur in $g(r)$ for the sample quenched from 140°C, and to a lesser extent for that quenched from 250°C (figure 6) and for orthorhombic S (figure 9).

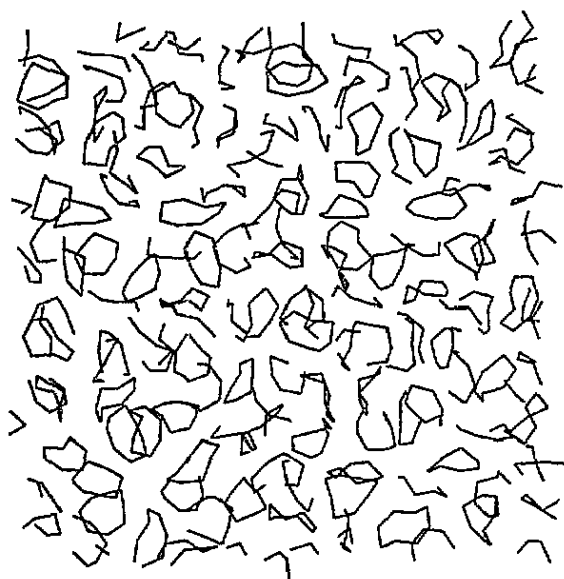


Figure 10. RMC results of model (ii) (flexible S_8 molecules) for liquid S at 140°C (note that all rings are perfectly connected, but some have been cut by taking a section for this figure).

So far all that has definitely been learned from RMC modelling is that the model (i) is not appropriate; the structural data do not contain enough information (by themselves)

to decide between many other possible models, but by looking in detail at the differences between models for different temperatures and phases we may learn something about the structural changes. This work is in progress.

5. Discussion

We have measured the structure factors of liquid and amorphous S for several states, in such a way that more highly resolved data on the pair correlation function could be obtained. These data demonstrate that some of the more popular models for some states of S need refinement, if they are to represent the observed distribution of molecular species. In particular the temperature dependence may have a more complicated origin than anticipated.

For example, a comparison of $g(r)$ of polymeric S with $g(r)$ of sulphur quenched from $T_q = 250^\circ\text{C}$ and with $g(r)$ of the parent liquid it was quenched from demonstrates that, although the latter two samples probably contain a large fraction of long S chains, no ordering of these chains occurs in the melt. It seems probable that S chains in the liquid are randomly dissolved in a liquid consisting of smaller S molecules.

As the local structural parameters of liquid S below and above the λ -transition temperature differ only very slightly, one might infer that the difference between these two regimes is only due to different sizes of 'molecular' units with similar local packing properties, and different thermal stabilities. Thus, it is possible that the high viscosity observed around $T \approx 159^\circ\text{C}$ could be due to a percolation limit being reached for these 'molecules'. However, this topic still requires more elaborate theoretical calculations.

Acknowledgment

We are happy to acknowledge the assistance of the staff of ISIS at the Rutherford Appleton Laboratory during the course of these experiments.

References

- [1] Meyer B 1965 *Elemental Sulfur* (New York: Interscience)
- [2] Meyer B 1976 *Chem. Rev.* **76** 367
- [3] Ruiz-Garcia J, Anderson E M and Greer S C 1989 *J. Phys. Chem.* **93** 6980
- [4] Steudel R and Mäusle H-J 1981 *Z. Anorg. (Allg.) Chem.* **478** 139
- [5] Thompson C W and Gingrich N S 1959 *J. Chem. Phys.* **31** 1598
- [6] Poltavtsev Yu G and Titenko Yu V 1975 *Russ. J. Phys. Chem.* **49** 178
- [7] Vahvaselka K S and Mangs J M 1988 *Phys. Scr.* **38** 737
- [8] Bellisent R, Descotes L, Boue F and Pfeuty P 1990 *Phys. Rev. B* **41** 2135
- [9] Winter R, Bodensteiner T, Szornel C and Egelstaff P A 1988 *J. Non-Cryst. Solids* **106** 100
- [10] Winter R, Szornel C, Pilgrim W-C, Howells W S and Egelstaff P A 1990 *J. Phys.: Condens. Matter* **2** 8427
- [11] Petschek R G, Pfeuty P and Wheeler J C 1986 *Phys. Rev. A* **34** 2391
- [12] Stillinger F H, Weber T A and La Violette R A 1986 *J. Chem. Phys.* **85** 6460
- [13] Malaurent J C and Dixmier J 1977 *Phys. Status Solidi a* **43** K61
- [14] Popescu M 1987 *J. Non-Cryst. Solids* **97 & 98** 187
- [15] Winter R, Pilgrim W-C, Egelstaff P A, Chieux P, Anlauf S, Hensel F 1990 *Europhys. Lett.* **11** 225
- [16] McGreevy R L and Howe M A 1992 *Annual Rev. Mater. Sci.* **22** 217